UDC 550.8
DOI: http://doi.org/10.17721/1728-2713.105.15

Vitalii ZATSERKOVNYI[1], DSc (Techn.), Prof.
ORCID ID: 0009-0003-5187-6125
e-mail: vitalii.zatserkovnyi@gmail.com

Irina TSIUPA[1], PhD (Geol.),
ORCID ID: 0000-0002-8350-6685
e-mail: irynatsiupa@knu.ua

Hryhorii OSTAPENKO[1], Stud.
ORCID ID: 0000-0003-0042-7437
e-mail: grishakelvin@gmail.com

Mauro DE DONATIS[2], PhD (Geol.), Assoc. Prof.
ORCID ID: 0000-0002-9721-1095
e-mail: mauro.dedonatis@uniurb.it

Leonid ILYIN[3], DSc (Geogr.), Prof.
ORCID ID: 0000-0002-4180-0544
e-mail: ilyinleo@ukr.net

[1]Taras Shevchenko National University of Kyiv, Kyiv, Ukraine
[2]University of Urbino Carlo Bo, Urbino, Italy
[3]Lesya Ukrainka Volyn National University, Lutsk, Ukraine

ANALYSIS OF THE CONSEQUENCES OF EARTHQUAKES IN TURKEY 06.02.2023 USING RADAR INTERFEROMETRY

(Представлено членом редакційної колегії д-ром геол. наук, проф. С.А. Вижвою)

Background. *The article studies the consequences of a series of earthquakes that occurred on February 6, 2023 in Turkey, which caused large-scale destruction and tens of thousands of victims, and became the deadliest in the world in the last 10 years. Research on the effects of earthquakes is important and can be used in emergency management and disaster recovery, to improve building standards, develop earthquake-resistant infrastructure, etc.*

Methods. *The study was performed using modern methods of remote sensing and geographic information systems. To quantify the surface displacement, we used the method of synthetic aperture interferometry (InSAR) based on Sentinel-1 satellite images in the SNAP application. To improve the accuracy of the results, the Goldstein filter was applied and the phase unwrapping was performed using the external Snaphu software module. To compensate for data distortion, terrain correction was performed using the Doppler terrain correction operator to make the geometric image as close to the real world as possible.*

Results. *The interferograms obtained before and after the earthquakes were analyzed. The results indicate significant surface deformations, especially in the area of the East Anatolian fault, with a maximum subsidence of 110 cm and more pronounced fault lines. The interferograms show that the earthquakes have caused significant changes in the fault structure, which may affect further seismic activity in the region. Diagrams and maps showing the impact of earthquakes on the surface and crust in the southeastern part of Turkey were constructed.*

Conclusions. *This study demonstrates the possibility of using InSAR technology to monitor the deformation of the earth's surface caused by recent earthquakes. The data obtained can be used to assess damage, identify risk areas, and develop measures to reduce seismic hazards.*

Keywords: *earthquake, Turkey, InSAR, Sentinel-1, deformation of the earth's surface, fault, seismic hazard.*

Background

The consequences of an earthquake can be devastating, leading to significant loss of life and material damage, especially in cities. Observing damaged buildings is critical for emergency management professionals as it helps them quickly direct rescue teams to the right location (Menderes, Erener, & Sarp, 2015).

The southeastern region of Turkey and northwestern Syria is a seismic zone characterized by a classical model of earthquake formation, where tectonic plates converge along fault lines, pressure gradually increases and provokes repeated tremors (Liu, 2023). Seismic activity in this area is influenced by such large structures as the North Anatolian fault (NAF), the East Anatolian fault (EAF) and the zone of the Southeast Anatolian depression (SAF) (Fotiou, 2023). Also, the susceptibility to the formation of earthquakes in this region is confirmed by the location in the contact zone of the Eurasian, African and Arabian plates (Seyitoğlu et al., 2017). The neotectonics of Southeast Turkey, northern Syria and Iraq have been widely studied, the causes of seismic processes in the region are three main tectonic elements – the North and East Anatolian fault zones, as well as the Aegean-Cyprus arc that separates the Anatolian plate from the Eurasian, Arabian and African plates (Gürbüz, 2020).

According to the Turkey Department of Earthquakes (AFAD), a series of earthquakes with the largest magnitudes 7.7 and 6.6 occurred in Turkey on February 6, 2023, about 29–33 km south of Kahramanmarash. These earthquakes occurred almost simultaneously (with a time difference of 10 minutes) at shallow depths (8.6 and 6.2 m, respectively). Seismic events have led to significant loss of life, destruction of infrastructure and caused a humanitarian crisis (Jia et al., 2023; Oduoye et al., 2023). The earthquake was the largest earthquake in Turkey since the 1939 Erzincan earthquake, indicating an increased risk throughout the region (Zhao et al., 2023). The earthquake was recorded by a large number of seismic stations, which gave a unique opportunity to study its characteristics and estimates of the destruction that occurred (Ding et al., 2023; Centre Sismologique Euro-Méditerranéen (CSEM)).

Problem Statement. Despite the great potential of remote sensing materials in the study of earthquakes at the beginning of the development of science, their use is limited mainly to structural-geological and geomorphological studies. These methods do not effectively measure short-term processes before and after seismic shocks.

Further development of remote sensing materials was associated with geophysical research. Over the past few

ISSN 1728-2713 (Print), ISSN 2079-9063 (Online)

decades, scientists have developed the ability to measure deformation on a centimeter scale by comparing satellite images taken at intervals of several days to several years. This ability has led to a significant increase in the percentage of the Earth's surface on which deformations and the frequency of such observations can be observed.

In the early 1990s, one powerful satellite method for estimating surface displacement became widely used – interferometric radar with a synthetic aperture (InSAR). Specifically, synthetic aperture radar (SAR) technology was used in the analysis of the aftermath of the 1999 Izmir earthquake in Turkey. SAR technology combined with interferometric coherence has been proposed to detect damage in buildings following the 1999 earthquake (Brunner, Lemoine, & Bruzzone, 2010). According to the authors, this technology can provide detailed descriptions of the consequences of the earthquake in Turkey in 2023, helping to assess the consequences of the destruction.

The aim of the work is to study the methods of remote sensing and geographic information systems of the consequences of a series of earthquakes in Turkey, in particular, to evaluate the existing methods of studying surface displacements that can be applied to this territory, to build diagrams and maps reflecting the impact of earthquakes on the surface and the earth's crust in Turkey. The conclusion of the work will be conclusions about the impact of earthquakes in the study area and analysis of risks that may be caused by tremors.

Analysis of recent researches and publications. The article (Bianchini et al., 2018) describes that InSAR, or synthesized aperture interferometric radar, is a technology that uses phase differences of two or more SAR images to measure the displacement of the Earth's surface to within centimeters and even millimeters (Bianchini et al., 2018). This method involves using complex satellite images of the territory obtained from different orbital positions and/or at different times to calculate the difference in distance to targets on the ground. The SAR signal phase is widely used to obtain information, and InSAR has been proven to be a valuable tool for mapping surface deformation with unprecedented spatial disparity (Bianchini et al., 2018).

The paper (Li et al., 2016) provides a comprehensive overview of the Sentinel-1 satellite mission developed by the European Space Agency (ESA), which revolutionized large-scale InSAR analysis through the use of C-band SAR images. Currently, the Sentinel-1 mission contains two satellites (S1A and S1B) launched in 2014 and 2016, respectively. These satellites serve as radar missions for InSAR applications, continuously collecting data in tectonic and volcanic areas around the world. In particular, the mission's ability to revisit the same site every 6-12 days meets the requirements of near-real-time global monitoring, enabling researchers to track geological processes with unprecedented frequency and accuracy.

The paper (Gaddes et al., 2018) notes that images from the Sentinel-1 satellite are used for synthetic aperture interferometric radar (InSAR) for almost real-time global monitoring. This is important for retrospective analysis and measurement of various phenomena, including earthquakes.

The time series analysis package of SAR interferometry with open code, LiCSBAS, integrates with the Sentinel-1 InSAR automated processor (COMET-LiCSAR) as described in the papers (Ghorbani et al., 2022; Dewanto, Setiawan, & Nusantara, 2020). These authors used Sentinel-1 satellite images to measure soil subsidence, climate change and other applications, including studying earthquakes.

A phase-deployment method was proposed in 2002 by Chen, & Zebker (2002) for synthesized aperture radar (SAR) interferograms. This method applies statistical segmentation and generalized network models to estimate unambiguous phase values from observed phase data, which are presented in the range of $-\pi$ to π. This method is main one for obtaining phase values from a two-dimensional phase array and converting phase values to standard units. The approach is to consider a larger interferogram as a mosaic of smaller interferograms (tiles) that can be unfolded sequentially. To solve the problem of combining tiles with a deployed phase, the authors propose a tile deployment scheme that extends the maximum posterior probability estimation system adopted by SNAPHU. The scheme is based on previously obtained models and develops a method for assembling individual unfolded tiles into the most probable full-size solution.

The work (Summerlin, 2022) describes the procedure for summarizing and drawing conclusions based on the technical part of the experiment to create InSar data. The author suggests using the standard set of SnAP functions to convert the results of the deployed phase into real data in centimeters for subsequent export and layout using GIS. The paper describes the use of Doppler correction when working with the expanded phase and bringing the image from the IW band format to geographical coordinates, taking into account angular corrections.

The study (Barut, Trinder, & Rizos, 2016) aimed to apply InSAR, GNSS and Coulomb stress modeling to post-seismic deformation analysis after the earthquake in Izmit, Turkey, held on 17 August 1999. The authors sought to understand the long-term effects of the earthquake and its implications for the earthquake cycle. The study described that observations of InSAR and GNSS in the three months after the earthquake, combined with simulations of Coulomb stress change, may explain the expansion of the fault zone as well as the deformation of the Northern NAF region. It was also found that there was a strong correspondence between InSAR and GNSS results for post-seismic study steps, with differences of less than 2 mm and a standard deviation of differences of less than 1 mm.

The territory of reserach. On the territory of Turkey there are tectonic boundaries of large geotectonic blocks: Eurasian, Arabian and Anatolian plates (fig. 1). The process of accumulation of tectonic stresses and subsequent movements along the tectonic boundaries, primarily the East Anatolian fault caused the occurrence of earthquakes on February 6, 2023. The East Anatolian fault zone is a plate boundary extending 500 km between the Arabian and Anatolian plates. The relative movement of the plates occurs with a sliding speed in the range of 6 to 10 mm/year, which creates a high risk of a new earthquake in eastern Turkey. In the area of Gaziantep and Kahramanmarash, the predicted peak ground accelerations for a probable earthquake can be 0.2–0.4 g (g – gravity acceleration 9.81 m/s^2), which correspond to a very destructive earthquake with an intensity of approximately 8–9 points. This is also evidenced by the map of the distribution of earthquake risks in the Middle East (fig. 2) (Korkmaz, 2009).

The East Anatolian fault, which is an intra-continental transform fault, is located in the Eastern Mediterranean region. Together with the right-sided North Anatolian fault, it contributes to the movement of the Anatolian microplate to the west. The fault is a complex left-sided landslide that separates the microplate from the Arabian Plate (Dal Zilio, & Ampuero, 2023).

Methods

InSAR is a method by which the phase difference of two or more SAR images is used to calculate the difference in range from two SAR antennas, which have slightly different geometry of vision, to targets on the ground. As a result, we get the value of the displacement of the surface for the given period exactly to centimeters. InSAR results provide an opportunity to evaluate deformations associated with faults, cracks and subsidence.

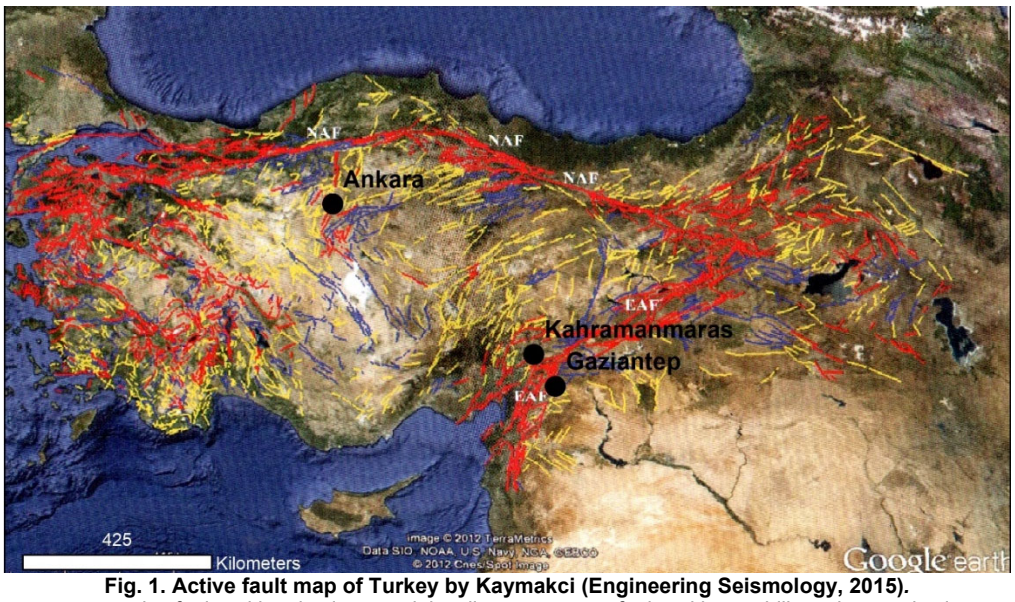

Fig. 1. Active fault map of Turkey by Kaymakci (Engineering Seismology, 2015).
Red represents active faults with seismic potential, yellow represents faults with capability to have seismic potential, blue represents faults with probability to have seismic potential. NAF – the North Anatolian right-lateral strike-slip fault zone. EAF – the East Anatolian left-lateral strike-slip fault zone

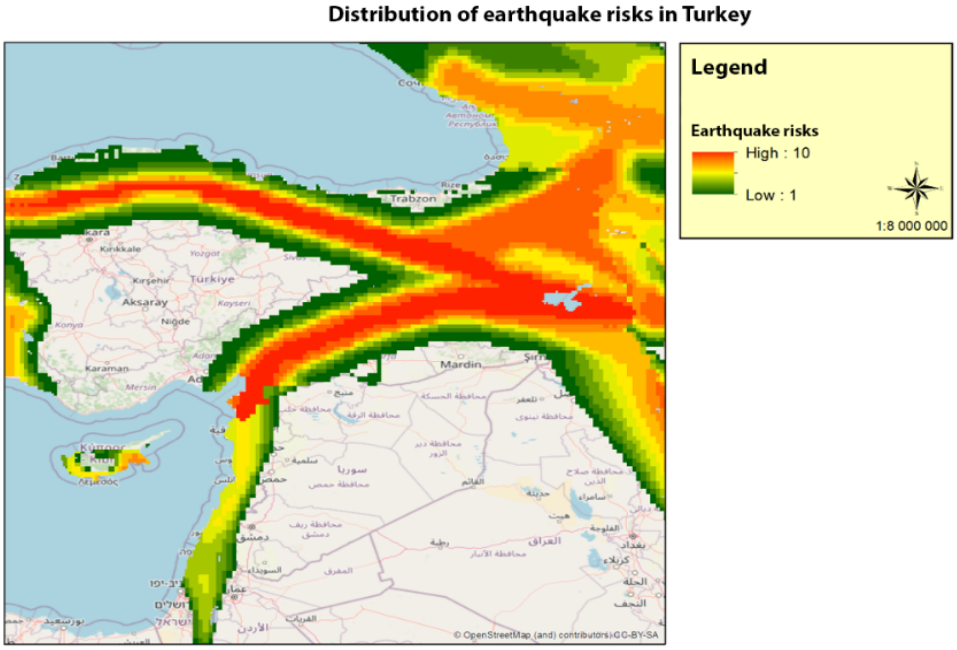

Fig. 2. The distribution of earthquake risks In Turkey (Korkmaz, 2009)

Radar, an abbreviation for radio detection and range determination, involves the transmission and reception of microwave electromagnetic radiation with frequencies in the range of approximately 108–1011 Hz and corresponding wavelengths of about 1–1000 mm (Rüeger, 2012).

The research utilizes Sentinel-1 data obtained from the Copernicus Open Access Hub, specifically focusing on the interferometric wide (IW) mode with a spatial resolution of 5 m by 20 m and polarized in VV+VH. This mode is the primary overland acquisition mode for Sentinel-1, covering a range of 250 km. The references provide valuable insights into the capabilities and applications of Sentinel-1 data (Nägler et al., 2015).

The Sentinel-1 satellite provides radar images in two directions: ascending and descending. These images differ in geometry and final characteristics, including the direction of the Doppler shift. In ascending mode, the Doppler shift is positive, indicating an increase in the frequency of the radar signal as the satellite approaches the target and a decrease as it moves away from it. Conversely, in the downshift mode,

the Doppler shift is negative, the radar signal frequency decreases as the satellite approaches the target and increases as it moves away (Moiseev et al., 2020; Karbou et al., 2021; Fan et al., 2023).

A Doppler shift is a change in frequency or wavelength relative to an observer that is moving relative to a wave source. In the context of InSAR imaging, Doppler terrain correction is necessary to account for geometric parameters of the InSAR system, including baseline length and slope, and to correct for atmospheric signal associated with terrain. Range Doppler Terrain Correction implements a Doppler terrain correction method for geocoding SAR images from two-dimensional raster radar geometry. It uses available information about the orbit state vector in metadata, radar time annotations, tilt-to-ground conversion parameters together with reference DTM data to obtain accurate geolocation information (Wang et al., 2023).

The use of terrain correction in InSAR imaging is particularly important because it corrects geometric distortions caused by topographic variations that can significantly affect the accuracy of the final image. Given the terrain and atmospheric effects, Doppler relief correction ensures that the InSAR image accurately reflects the features of the observation surface, which leads to more reliable results in applications such as topographic mapping, monitoring of soil deformation, and detection of changes in the environment (Wang et al., 2023).

The S-1 uses three predefined subbands in IW mode (IW1, IW2 and IW3), reaching a coverage of 250 km in the transverse direction. To do this, it uses advanced SAR scanning terrain observation technology (TOPSAR). This allows for electronic beam control in both the rangefinder and azimuthal directions, ensuring the same image quality over the entire range and avoiding jagged images (Yague-Martinez et al., 2016). TOPSAR is designed to replace ScanSAR mode and provide an almost uniform signal-to-noise ratio (SNR) and distributed target ambiguity ratio (DTAR) (Yague-Martinez et al., 2016). The IW TOPSAR mode provides highly accurate and nearly uniform responses when images are co-recorded, eliminating flaws that reduce the azimuth antenna emission pattern seen by the ground target. In addition, the IW mode supports single and double polarization operation, covering a range of incidence angles from 31 to 46 degrees (Ouaadi et al., 2021).

Table 1

Characteristics of satellite data Sentinel-1 (Prats-Iraola et al., 2015)

Parameter	Interferometric Wide-swath mode (IW)
Polarization	Dual (HH+HV, VV+VH)
Access (angles of incidence)	31°– 46°
Azimuth mismatch	<20 m
Ground Range Mismatch	<5 m
Azimuth and range view	Single
Strip	>250 km
Maximum NESZ	−22dB
Radiometric stability	0.5 dB(3σ)
Radiometric accuracy	1 dB (3σ)
Phase Error	5°

After loading Sentinel-1 data into the SNAP application, a number of steps must be taken to create an interferogram. These actions are represented by the following program tools: Apply Orbit File, Back-Geocoding, Enhanced Spectral Diversity, Interferogram, and TOPSAR-Deburst.

Apply Orbit File – Auxiliary orbit data contains information about the position of the satellite when receiving SAR data. They are automatically loaded for Sentinel-1 SNAP products and added to their metadata using the Apply Orbit File statement.

Back Geocoding – The reverse geocoding tool S-1 jointly registers two separated products based on the orbit information added in the previous step and information from the digital altitude model (DEM) that SNAP loads.

Enchanted Spectral Diversity is a method proposed to solve the problem of azimuthal displacement caused by misalignment of Sentinel-1A/B data in the process of monitoring large-scale deformations. This method uses spectral diversity for the overlap region between TOPS data packets and involves two stages of joint data registration: initial joint registration based on geometry and subsequent joint registration using ESD. The main goal of ESD is to achieve a co-registration accuracy of about 0.001 pixels to limit the azimuthal shift to several degrees (Wang, Xu, & Fialko, 2017).

The interferogram is formed by cross-multiplying (formula 1-4) the reference image by the complex conjugation of the secondary image. The amplitude of both images is multiplied and the phase represents the phase difference between the two images. The interferometric phase of each pixel of the SAR image will depend only on the difference in paths from each of the two SARs to the disparity cell under observation.

$$\varphi = \varphi_{DEM} + \varphi_{\text{flat}} + \varphi_{\text{disp}} + \varphi_{\text{atm}} + \varphi_{\text{noise}} \quad (1)$$

$$\varphi_{\text{flat}} = -\frac{4\pi}{\lambda} \cdot \frac{B_n \cdot s}{R \cdot \tan\theta} \quad (2)$$

$$\varphi_{DEM} = \frac{4\pi}{\lambda} \cdot \frac{B_n}{R_0} \cdot \frac{\Delta\varphi}{\sin\theta} \quad (3)$$

$$\varphi_{\text{disp}} = d \cdot \frac{4\pi}{\lambda} \quad (4)$$

Accordingly, the calculated interferogram takes into account the flat earth phase φ flat (curvature of the earth), topographic phase φ DEM (topographic surface of the earth), atmospheric conditions φ atm (change in humidity, temperature and pressure between the two gains) and other noise φ noise (change in scatterers, different viewing angle and volume scattering), and finally possible surface deformation φ disp, which occurred between the two preparations (Vrankić, Grgić, & Bašić, 2022). TOPSAR-Deburst is a function for merging individual IW image strips into one.

The interferometric phase most often contains noise and distortion from temporal and geometric decorrelation, bulk scattering and other processing errors. Phase information in the de-correlated regions cannot be recovered, but the quality of the bands present on the interferogram can be improved by applying specialized phase filters such as the Goldstein filter to improve the signal-to-noise ratio.

$$H(f_x, f_y) = S\{|Z(f_x, f_y)|\}^a * Z(f_x, f_y), \quad (5)$$

where fx and fy respectively represent the spatial frequencies in the range and azimuth α is the filter parameter, Z(fx, fy) represents the Fourier spectrum of each filtering window, and S{·} is the smoothing operator that is

usually achieved with a low-pass filter. Spots are defined as small windows of an interferogram with overlap to maintain continuity at the boundaries. The α parameter, taking the value in the range [0, 1], indicates the desired level of efficiency of the filtering operation. For α = 0, we have H(fx, fy) = Z(fx, fy), which means no filtering (Feng et al., 2016).

In order to relate the interferometric phase to the topographic relief on the interferogram, the phase difference between adjacent pixels is integrated, allowing the actual relief changes to be measured (Matano, 2019). The phase deployment required for this process is typically performed using external software such as SNAPHU, which uses a network flow algorithm to find the most likely expanded values. In addition, the interferometric phase is derived on the basis of first-order MNCs using adaptive window size, and the interferogram is pre-processed by filtration to eliminate strong noise that can cause serious errors (Sun et al., 2020).

Two-dimensional phase unfolding is the process of recovering unambiguous phase data from a two-dimensional array of phase values known only modulo 2pi rad. SNAPHU is an implementation of the statistical cost algorithm and network flow for phase deployment proposed by Chen and Zebker (2002). This algorithm sets the phase deployment as a maximum posterior probability (MAP) estimation problem, the purpose of which is to calculate the most probable deployed solution from the observed input data. Since the statistics that relate the input data to the solution depend on the measured quantity, SNAPHU contains three built-in statistical models: for topography data, deformation data, and smooth general data (Chen et al., 2018).

An important step in determining the amount of soil deformation is to quantify the results of the expanded phase as a total displacement. The expanded phase represents the cumulative phase difference between SAR images and needs to be converted to an offset value for further analysis. To do this, the pixel equation is used, which takes into account the delta phase and the wavelength of the sensor, to calculate the total displacement in meters.

Results

This research will analyze and study the territory (fig. 3) of southeastern Turkey, the area through which the East Anatolian Fault passes – a large fault zone that forms a transform-type tectonic boundary between the Anatolian Plate and the northward-moving Arabian Plate.

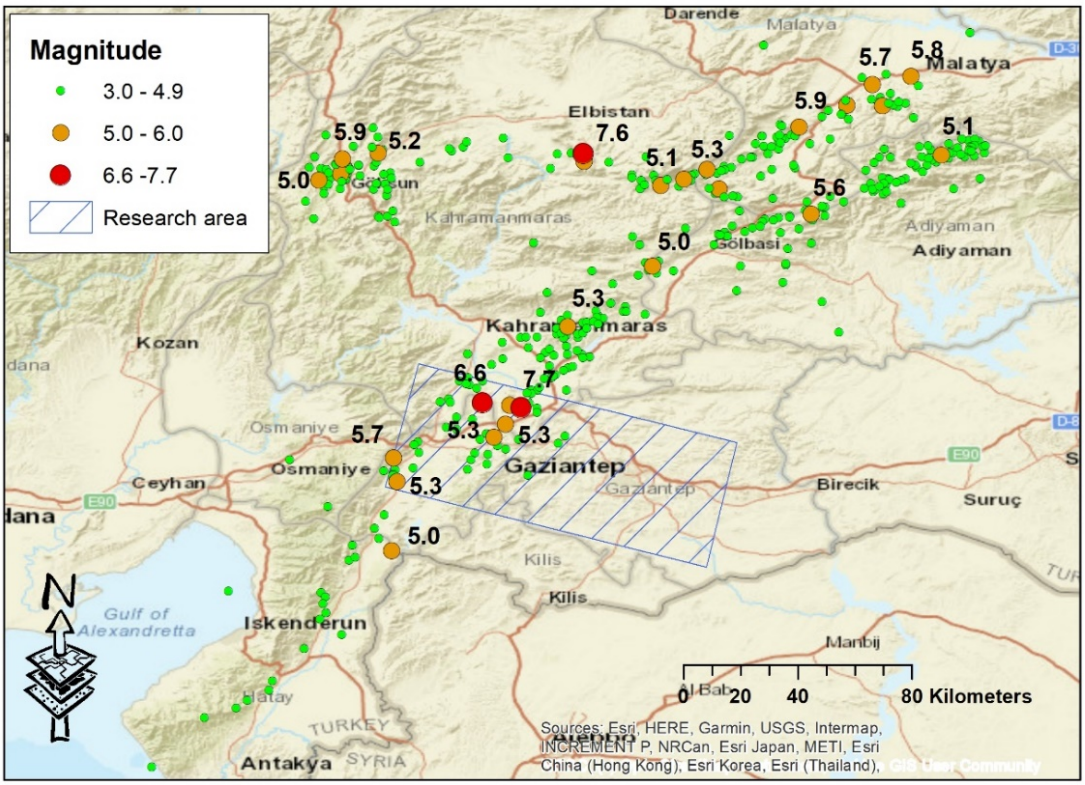

Fig. 3. Seismic events in Turkey 02/06/2023 (according to AFAD data)

In this research, we used data containing intensity and phase information, covering a width of 250 km in the interferometric wideband (IW) mode with a spatial resolution of 5 m by 20 m and polarized in VV+VH. The pre-earthquake datasets were acquired on January 17, 2023 and January 29, 2023, a week before the earthquake, and the post-earthquake dataset was acquired on February 10, 2023, 4 days after the earthquake (table 2).

Work with snapshots is done in the SNAP application. In order to obtain accurate results, in the process of processing radar interferometry data, two interferograms were obtained (fig. 4), which contain information on the deformation of the Earth's surface. However, these interferograms must be corrected at the output, since they may contain errors caused by atmospheric noise, as well as random measurements.

They were then corrected using the Goldstein filtration method. This stage will create the final version of the interferogram in the range from $-\pi$ to π (fig. 4). Further actions will be related to the phase sweep and obtaining the numerical values of the surface displacement in real units of measurement.

The phase is deployed using an external Snaphu software module. The expanded phase offset data is presented in its own units of measure, so to interpret them in meters, it is necessary to quantify the results of the expanded phase as a

total offset. To do this, the pixel equation was used, which takes into account the delta phase and the wavelength of the sensor, to calculate the total displacement in meters. The result is two images showing the displacement of the surface before and after the earthquake.

The measurement methods used showed displacement as a result of seismic shock and numerous secondary shocks after it. Displacements are located in the area of the East Anatolian fault, which has deep linear faults (fig. 5).

Table 2

Characteristics of the images

Date	Type	Polarization mode	Band	Time difference
January 17, 2023	SLC	VV + VH	C	12 days
January 29, 2023	SLC	VV + VH	C	
February 10, 2023	SLC	VV + VH	C	12 days

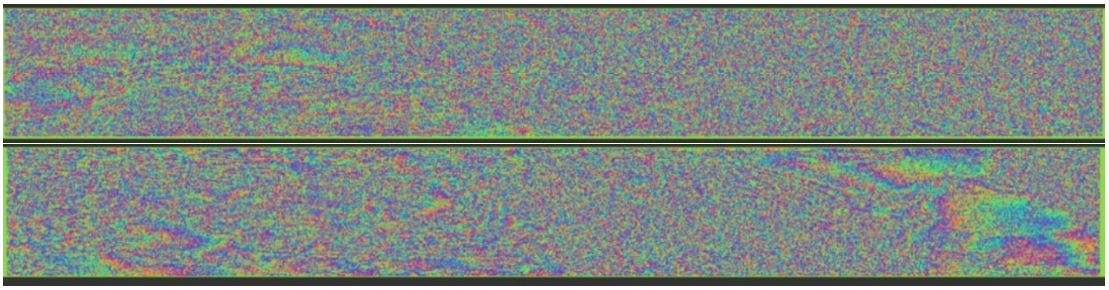

Fig. 4. Interferogram constructed from data from 17.01 to 29.01 (a), from 29.01 to 10.02 (b)

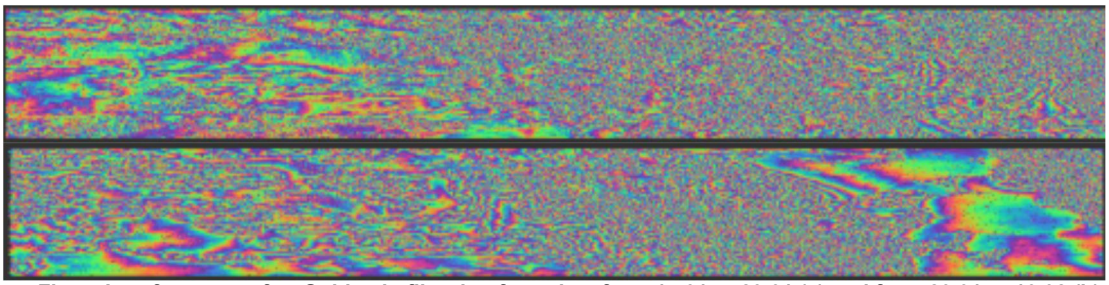

Fig. 5. Interferogram after Goldstein filtration from data from 17.01 to 29.01 (a) and from 29.01 to 10.02 (b)

East from the main epicenter of the earthquake expressed subsidence of the surface up to ±50 cm. Fault break lines are visible on the resulting interferograms and cover a significant spatial range along the fault. The results of the study indicate the impact of the earthquake on the structure of the fault and can be used for further analysis of its behavior. If we compare the displacement of the surface before the earthquake and after (fig. 6), we can see that the displacements before the earthquake are insignificant, with an amplitude of 30 cm, with minor subsidence up to 7 cm. After the earthquake, the amplitude of subsidence is up to 110 cm, and the fault line becomes clearly expressed.

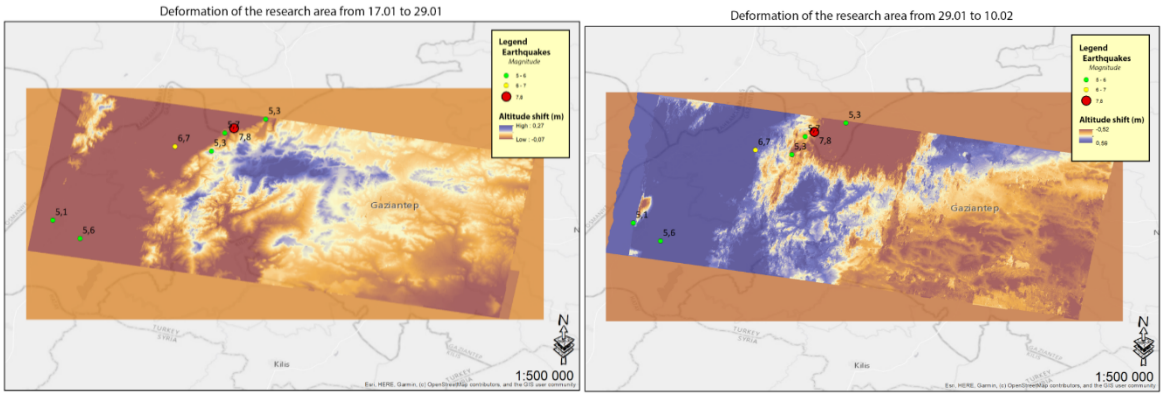

a **b**

Fig. 6. Displacement of the surface of the territory during the time from 17.01 to 29.01 (a) and from 29.01 to 10.02 (b)

Discussion and conclusions

The research included a detailed study of the consequences of a series of earthquakes in Turkey using modern remote sensing methods and geographic information systems. To obtain accurate data on surface displacement as a result of seismic events, Sentinel-1 satellite data processed in SNAP software was used and interferograms were created. To improve the accuracy of the results, a Goldstein filter was applied and the phase was deployed using an external Snaphu software module.

ISSN 1728-3817

The results of the study showed that the greatest surface displacements were found in the area of the East Anatolian fault, with a maximum surface subsidence of up to 110 cm. In addition, it was found that earthquakes caused significant changes in the structure of the fault, which may affect further seismic activity in the region.

The results obtained are important for further analysis of fault behavior and assessment of risks associated with seismic activity in the region. Also, the application of InSAR technology has provided important information about the consequences of earthquakes in Turkey and can be a useful tool for monitoring seismic activity and assessing risks in other regions of the world.

Thus, this study confirms the importance of using modern technologies to monitor and study the effects of seismic activity, as well as to develop effective strategies for risk reduction and disaster mitigation.

Authors' contribution: Vitalii Zatserkovnyi – conceptualization, methodology, editing; Irina Tsiupa – creating models, data validation, writing (revision and editing); Hryhorii Ostapenko – methodology, creating models, formal analysis, writing (original draft); Mauro De Donatis – writing (revision), data validation; Leonid Ilyin – editing, data validation.

References

Barut, R., Trinder, J., & Rizos, C. (2016). Analysing post-seismic deformation of izmit earthquake with insar, gnss and coulomb stress modelling. *The International Archives of the Photogrammetry Remote Sensing and Spatial Information Sciences,* XLI-B1, 417–421. https://doi.org/10.5194/isprsarchives-xli-b1-417-2016

Bianchini, S., Raspini, F., Solari, L., Soldato, M., Ciampalini, A., & Rosi, A. (2018). From picture to movie: twenty years of ground deformation recording over tuscany region (italy) with satellite insar. *Frontiers in Earth Science*, 6. https://doi.org/10.3389/feart.2018.00177

Brunner, D., Lemoine, G., & Bruzzone, L. (2010). Earthquake damage assessment of buildings using vhr optical and sar imagery. *Ieee Transactions on Geoscience and Remote Sensing,* 48(5), 2403–2420. https://doi.org /10.1109/tgrs.2009.2038274

Centre Sismologique Euro-Méditerranéen – Euro-Mediterranean Seismological Centre. https://www.emsc-csem.org/Earthquake_map/

Chen, C., & Zebker, H. (2002). Phase unwrapping for large sar interferograms: statistical segmentation and generalized network models. *Ieee Transactions on Geoscience and Remote Sensing,* 40(8), 1709–1719. https://doi.org/10.1109/tgrs.2002.802453

Chen, Q., Li, T., Tang, X., Gao, X., & Zhang, X. (2018). Preliminary gaofen-3 insar dem accuracy analysis. *The International Archives of the Photogrammetry Remote Sensing and Spatial Information Sciences*, XLII-3, 173–177. https://doi.org/10.5194/isprs-archives-xlii-3-173-2018

Dal Zilio, L., & Ampuero, J. P. (2023). Earthquake doublet in Turkey and Syria. *Commun Earth Environ* 4, 71 https://doi.org/10.1038/s43247-023-00747-z

Dewanto, B., Setiawan, M., & Nusantara, G. (2020). Opak fault deformation monitoring using sentinel-1 insar data from 2016-2019 in yogyakarta indonesia. *Elipsoida Jurnal Geodesi Dan Geomatika,* 3(01), 46–54. https://doi.org/10.14710/elipsoida.2020.7758

Ding, X., Xu, S., Xie, Y., Ende, M., Premus, J., & Ampuero, J. (2023). The sharp turn: backward rupture branching during the 2023 mw 7.8 turkey earthquake. https://doi.org/10.21203/rs.3.rs-3163216/v1

Engineering Seismology with Applications to Geotechnical Engineering (2015). Öz Yilmaz. *Investigation in Geophysics series,* No.17. USA. ISBN 078-0-931830-46-4

Fan, S., Zhang, B., Moiseev, A., Kudryavtsev, V., Johannessen, J., & Chapron, B. (2023). On the use of dual co-polarized radar data to derive a sea surface doppler model—part 2: simulation and validation. *Ieee Transactions on Geoscience and Remote Sensing*, 61, 1–9. https://doi.org/10.1109/tgrs.2023.3246771

Feng, Q, Xu, H, Wu, Z, You, Y, Liu, W, & Ge, S. (2016). Improved Goldstein Interferogram Filter Based on Local Fringe Frequency Estimation. *Sensors*, 16(11):1976. https://doi.org/10.3390/s16111976

Fotiou, K. (2023). *Impact assessment of the catastrophic earthquakes of 6 february 2023 in turkey and syria via the exploitation of satellite datasets*. https://doi.org/10.1117/12.2682926

Gaddes, M., Hooper, A., Bagnardi, M., Inman, H., & Albino, F. (2018). Blind signal separation methods for insar: the potential to automatically detect and monitor signals of volcanic deformation. *Journal of Geophysical Research Solid Earth*, 123(11). https://doi.org/10.1029/2018jb016210

Ghorbani, Z., Khosravi, A., Maghsoudi, Y., Mojtahedi, S., Javadnia, E., & Nazari, A. (2022). Use of insar data for measuring land subsidence induced by groundwater withdrawal and climate change in ardabil plain, iran. *Scientific Reports*, 12(1). https://doi.org/10.1038/s41598-022-17438-y

Gürbüz, A. (2020). Quaternary Tectonics as the Neotectonics in Turkey. *Geotecton.*, 54, 797–806. https://doi.org/10.1134/S0016852120060060

Jia, Z., Jin, Z., Marchandon, M., Ulrich, T., Gabriel, A.-A., Fan, W., Shearer, P., Zou, X., Rekoske, J., … & Fialko, Y. (2023). The complex dynamics of the 2023 kahramanmaraş, turkey,mw 7.8–7.7 earthquake doublet. *Science*, 381(6661), 985–990. https://doi.org/10.1126/science.adi0685

Karbou, F., Veyssière, G., Coléou, C., Dufour, A., Gouttevin, I., Durand, P., … & Grizonnet, M. (2021). Monitoring wet snow over an alpine region using sentinel-1 observations. *Remote Sensing*, 13(3), 381. https://doi.org/10.3390/rs13030381

Korkmaz, K.A. (2009). Earthquake disaster risk assessment and evaluation for Turkey. *Environmental Geology*, 57, 307–320. https://doi.org/10.1007/s00254-008-1439-1

Li, Z., Wright, T., Hooper, A., Crippa, P., González, P., Walters, R., … & Parsons, B. (2016). Towards insar everywhere, all the time, with sentinel-1. *The International Archives of the Photogrammetry Remote Sensing and Spatial Information Sciences*, XLI-B4, 763–766. https://doi.org/10.5194/isprs-archives-xli-b4-763-2016

Liu, C. (2023). Complex multi-fault rupture and triggering during the 2023 earthquake doublet in southeastern türkiye. *Nature Communications,* 14(1). https://doi.org/10.1038/s41467-023-41404-5

Matano, F. (2019). Analysis and classification of natural and human-induced ground deformations at regional scale (Campania, Italy) detected by satellite synthetic-aperture radar interferometry archive datasets. *Remote Sensing*, 11(23), 2822.

Menderes, A., Erener, A., & Sarp, G. (2015). Automatic detection of damaged buildings after earthquake hazard by using remote sensing and information technologies. Procedia Earth and Planetary Science, 15, 257–262. https://doi.org/10.1016/j.proeps.2015.08.063

Moiseev, A., Johnsen, H., Hansen, M., & Johannessen, J. (2020). Evaluation of radial ocean surface currents derived from sentinel-1 iw doppler shift using coastal radar and lagrangian surface drifter observations. *Journal of Geophysical Research Oceans*, 125(4). https://doi.org/10.1029/2019jc015743

Nägler, T., Rott, H., Hetzenecker, M., Wuite, J., & Potin, P. (2015). The sentinel-1 mission: new opportunities for ice sheet observations. *Remote Sensing*, 7(7), 9371–9389. https://doi.org/10.3390/rs70709371

Oduoye, M., Nazir, A., Gharaibeh, R., Yoruk, E., Sulakci, A., Nafula, W., … & Akilimali, A. (2023). Devastating earthquake in turkey: a call for global action. *International Journal of Surgery Global Health*, 6(2), e128–e128. https://doi.org/10.1097/gh9.0000000000000128

Ouaadi, N., Ezzahar, J., Khabba, S., Er-Raki, S., Chakir, A., Ait Hssaine, B., Le Dantec, V., Rafi, Z., Beaumont, A., Kasbani, M., & Jarlan, L. (2021). C-band radar data and in situ measurements for the monitoring of wheat crops in a semi-arid area (center of Morocco), *Earth Syst. Sci. Data*, 13, 3707–3731. https://doi.org/10.5194/essd-13-3707-2021

Prats-Iraola, P., Nannini, M., Scheiber, R., De Zan, F., Wollstadt, S., Minati, F., ... & Desnos, Y. L. (2015, July). Sentinel-1 assessment of the interferometric wide-swath mode. In 2015 IEEE international geoscience and remote sensing symposium (IGARSS) (pp. 5247–5251). IEEE. https://doi.org/10.1109 /IGARSS.2015.7327018

Rüeger, J. M. (2012). *Electronic distance measurement:* An introduction. Springer Science & Business Media. https://doi.org/10.1007/978-3-642-80233-1

Seyitoğlu, G., Esat, K., & Kaypak, B. (2017). The neotectonics of southeast turkey, northern syria, and iraq: the internal structure of the southeast anatolian wedge and its relationship with recent earthquakes. *Turkish Journal of Earth Sciences*, 26, 105–126. https://doi.org/10.3906/yer-1605-21

Summerlin, T. (2022). *Measuring Ground Deformation Using Interferometry*. http://hdl.handle.net/10150/665583

Sun, X., Zimmer, A., Mukherjee, S., Kottayil, N. K., Ghuman, P., & Cheng, I. (2020). DeepInSAR–A deep learning framework for SAR interferometric phase restoration and coherence estimation. *Remote Sensing*, 12(14), 2340.

Turkey Department of Eearthquake (AFAD). https://tdvms.afad.gov.tr /event_spec_data

Vrankić, M., Grgić, M., & Bašić, T. (2022). Monitoring of geophysical processes in the area of western Herzegovina by satellite observations. *Electronic Collection of Papers of the Faculty of Civil Engineering*, (23). https://doi.org/10.47960/2232-2022.23.12.36

Wang, K., Xu, X. & Fialko, Yu. (2017). Improving Burst Alignment in TOPS Interferometry With Bivariate Enhanced Spectral Diversity. *IEEE Geoscience and Remote Sensing Letters*. PP. 1–5. 10.1109/LGRS.2017.2767575.

Wang, Z., Zhang, W., Taymaz, T., He, Z., Xu, T., & Zhang, Z. (2023). Dynamic rupture process of the 2023 Mw 7.8 Kahramanmaraş earthquake (SE Türkiye): Variable rupture speed and implications for seismic hazard. *Geophysical Research Letters*, 50, e2023GL104787. https://doi.org/10.1029 /2023GL104787

Yague-Martinez, N., Prats-Iraola, P., González, F., Brcic, R., Shau, R., Geudtner, D., … & Bamler, R. (2016). Interferometric processing of sentinel-1 tops data. *Ieee Transactions on Geoscience and Remote Sensing*, 54(4), 2220–2234. https://doi.org/10.1109/tgrs.2015.2497902

Zhao, J., Chen, Q., Yang, Y., & Xu, Q. (2023). Coseismic faulting model and post-seismic surface motion of the 2023 Turkey–Syria earthquake doublet revealed by insar and gps measurements. *Remote Sensing*, 15(13), 3327. https://doi.org/10.3390/rs15133327

Отримано редакцією журналу / Received: 10.12.23
Прорецензовано / Revised: 01.03.24
Схвалено до друку / Accepted: 29.05.24

Віталій ЗАЦЕРКОВНИЙ[1], д-р техн. наук, проф.
ORCID ID: 0009-0003-5187-6125
e-mail: vitalii.zatserkovnyi@gmail.com

Ірина ЦЮПА[1], канд. геол. наук
ORCID ID: 0000-0002-8350-6685
e-mail: irynatsiupa@knu.ua

Григорій ОСТАПЕНКО[1], студент
ORCID ID: 0000-0003-0042-7437
e-mail: grishakelvin@gmail.com

Мауро ДЕ ДОНАТІС[2], д-р філософії, доц.
ORCID ID: 0000-0002-9721-1095
e-mail: mauro.dedonatis@uniurb.it

Леонід ІЛЬЇН[3], д-р геогр. наук, проф.
ORCID ID: 0000-0002-4180-0544
e-mail: ilyinleo@ukr.net

[1]Київський національний університет імені Тараса Шевченка, Київ, Україна
[2]Університет Урбіно Карло Бо, Урбіно, Італія
[3]Волинський національний університет імені Лесі Українки, Луцьк, Україна

АНАЛІЗ НАСЛІДКІВ ЗЕМЛЕТРУСІВ У ТУРЕЧЧИНІ 06.02.2023 ЗА ДАНИМИ РАДІОЛОКАЦІЙНОЇ ІНТЕРФЕРОМЕТРІЇ

В с т у п . ***Досліджено наслідки серії землетрусів, що відбулись 6 лютого 2023 року в Туреччині та спричинили масштабні руйнування й десятки тисяч жертв, а також стали найбільш смертоносними у світі за останні 10 років. Дослідження наслідків землетрусів мають важливе значення і можуть використовуватися у сфері управління надзвичайними ситуаціями та відновленні після природних катастроф, а також для поліпшення будівельних стандартів, розробки інфраструктури більш стійкої до землетрусів тощо.***

М е т о д и . ***Дослідження виконано за допомогою сучасних методів дистанційного зондування та геоінформаційних систем. Для кількісної оцінки зміщення поверхні використано метод інтерферометрії із синтезованою апертурою (InSAR) на основі космічних знімків супутника Sentinel-1 у застосунку SNAP. Для підвищення точності результатів застосовувався фільтр Гольдштейна та виконано розгортання фази за допомогою зовнішнього програмного модуля Snaphu. Для компенсації спотворень даних здійснено корекцію місцевості за допомогою оператора Doppler Terrain Correction, щоб геометричне зображення було максимально наближеним до реального.***

Р е з у л ь т а т и . ***Проаналізовано інтерферограми, отримані до та після землетрусів. Результати свідчать про значні деформації поверхні, особливо в районі Східноанатолійського розлому, з максимальним просіданням 110 см та більш вираженими лініями розлому. За даними інтерферограм можна дослідити, що землетруси спричинили значні зміни у структурі розлому, що може вплинути на подальшу сейсмічну активність у регіоні. Виконано побудову схем та карт, що відображають вплив землетрусів на поверхню та земну кору в південно-східній частині Туреччини.***

В и с н о в к и . ***Дослідження демонструє можливості використання технології InSAR для моніторингу деформацій земної поверхні, спричинених нещодавніми землетрусами. Отримані дані можуть бути використані для оцінки руйнувань, визначення зон ризику та розробки заходів щодо зниження сейсмічної небезпеки.***

К л ю ч о в і с л о в а : ***землетрус, Туреччина, InSAR, Sentinel-1, деформація земної поверхні, розлом, сейсмічна небезпека.***

Автори заявляють про відсутність конфлікту інтересів. Спонсори не брали участі в розробленні дослідження; у зборі, аналізі чи інтерпретації даних; у написанні рукопису; в рішенні про публікацію результатів.

The authors declare no conflicts of interest. The funders had no role in the design of the study; in the collection, analyses or interpretation of data; in the writing of the manuscript; in the decision to publish the results.